Journal of Applied Physics ARTICLE scitation.org/journal/jap

Charge-independent protein adsorption characteristics of epitaxial graphene field-effect transistor on SiC substrate

Cite as: J. Appl. Phys. **130**, 074502 (2021); doi: 10.1063/5.0054688
Submitted: 21 April 2021 · Accepted: 31 July 2021 ·
Published Online: 16 August 2021

Hiroki Nakai,[1,a)] Daiu Akiyama,[1] Yoshiaki Taniguchi,[1] Iori Kishinobu,[1] Hiromichi Wariishi,[1] Yasuhide Ohno,[2,b)] Masao Nagase,[2] Takuya Ikeda,[3] Atsushi Tabata,[3,4] and Hideaki Nagamune[3,4]

AFFILIATIONS

[1]Graduate School of Advanced Technology and Science, Tokushima University, Tokushima, Tokushima 770-8506, Japan
[2]Institute of Post LED Photonics, Tokushima University, Tokushima, Tokushima 770-8506, Japan
[3]Graduate School of Sciences and Technology for Innovation, Tokushima University, Tokushima, Tokushima 770-8506, Japan
[4]Graduate School of Technology, Industrial and Social Sciences, Tokushima University, Tokushima, Tokushima 770-8513, Japan

[a)]**Electronic mail:** h_nakai@ee.tokushima-u.ac.jp
[b)]**Author to whom correspondence should be addressed:** ohno@ee.tokushima-u.ac.jp

ABSTRACT

Charge-independent biomolecule detection using field-effect transistors (FETs) with single-crystal and large-area epitaxial graphene films fabricated on SiC substrates is demonstrated. To obtain clean graphene channel surfaces, FETs were fabricated using stencil mask lithography, which is a resist-free fabrication process. Proteins with various isoelectric points (pI: 5.6–9.9) were used as targets. Transfer characteristics [drain current (I_D) vs solution-gate voltage (V_G) characteristics] were measured by changing the pH of the buffer solution. The I_D–V_G characteristics exhibited a clear negative gate voltage shift for both positively and negatively charged proteins, indicating that the epitaxial graphene FETs could not detect the charge type of the protein and electrons were doped by the adsorption of both positively and negatively charged proteins. These results cannot be explained by conventional electrostatic effects. Therefore, it can be concluded that the detection of biomolecules by the epitaxial graphene FETs occurred through charge transfer from the proteins. Moreover, the dissociation constants between the proteins and epitaxial graphene films were as small as 100 pM, indicating the high sensitivity of the graphene FETs.

I. INTRODUCTION

In recent years, lifestyle-related diseases have contributed to an increasing number of deaths and become a critical issue in many advanced countries. Numerous diagnostic methods have been developed for the early diagnosis of these diseases. Generally, highly sensitive and reliable optical detection methods, such as enzyme-linked immunosorbent assay (ELISA), are used for the detection of specific biomolecules. However, they require expensive apparatus and trained professionals who are knowledgeable about labeling processes, fluorescent dyes, and complex experimental techniques. Therefore, the development of low-cost, simple, highly sensitive, and user-friendly biosensors is desired.

Graphene is a two-dimensional crystal with a honeycomb structure of carbon atoms. Owing to the specific characteristics associated with its unique structure, it has the potential for numerous applications.[1–5] In particular, the extraordinary carrier mobility, chemical stability, and large specific surface area of graphene have driven studies on graphene-based sensors.[6–16] Numerous studies on biomolecule detection using graphene field-effect transistors (FETs) have been reported. The change in the transfer characteristics of these FETs resulting from biomolecule adsorption onto the graphene film has been attributed to two mechanisms, namely, the electrostatic effect[12,13,15] and the charge transfer effect.[14,17–20] In the electrostatic effect, charge carriers with an opposite sign from the biomolecule charge are induced in the graphene channel (e.g., a negatively charged protein inducing holes),[12,13,15] whereas in the charge transfer effect, carriers with the same sign as the biomolecule charge are induced (e.g., a negatively charged protein inducing electrons).[14,20] The inherent mechanism in graphene-based biosensors remains to

be clarified because several factors such as defects, dislocations, charged impurities in the insulator, contact resistance, and polymer residues are also suspected to influence the transfer characteristics. Therefore, although graphene-based biosensors are highly sensitive, they often exhibit incongruous characteristics. For instance, the direction of the shift in the drain current (I_D) vs solution gate voltage (V_G) characteristics has changed after the introduction of biomolecules. Moreover, the shift direction sometimes varies even when the same protein is introduced.[13,15] Although the current values depend on the quality of the graphene film, the difference in the shift directions indicates that the sensing mechanism has changed completely. Moreover, such unstable I_D–V_G shift characteristics may lead to unstable sensing results and decrease the reliability of the graphene-based sensor. To realize the practical use of graphene film-based sensing devices, it is crucial to understand their inherent characteristics, as a reference standard for graphene-based sensors. In FET-based biosensing, the electrical characteristics are affected by both the protein-specific binding to receptors and the non-specific protein binding to the channel. It is important to understand the behavior of both bare graphene and receptor-modified graphene FETs because the data for bare graphene FETs can be helpful for engineering non-specific protein adsorption for the development of receptor functionalization processes. Moreover, to overcome the problems caused by methods involving transfer processes, a resist-free fabrication method for the preparation of graphene FETs from single-crystal graphene films is required.

An epitaxial graphene film synthesized on a SiC substrate is a single crystal with large areas on the insulating substrate and does not require a transfer process.[21–23] Therefore, we can expect that the inherent sensing characteristics of only the graphene-based sensor are observed without the influence of the other factors mentioned above. It was recently shown that an epitaxial graphene FET cannot detect ions,[24] which suggests that the use of an epitaxial graphene FET has high potential for obtaining the inherent sensing characteristics of graphene-based sensors. However, the number of reports on biological sensor applications based on epitaxial graphene FETs is lower than those of sensors based on graphene synthesized via mechanical exfoliation, graphene oxide reduction (rGO), and chemical vapor deposition (CVD) growth. In this study, we investigate the pH dependence of various protein adsorption characteristics using a bare epitaxial graphene film on a SiC substrate. The device was fabricated by stencil mask lithography, which is a resist-free process, and the electrical measurements were carried out by four-terminal measurements to avoid the influence of the contact resistance.

II. EXPERIMENTAL METHODS

A. Materials

The pH-adjusted buffer solutions were prepared as follows: for pH 4.0–5.5 solutions, a 10 mM acetate buffer solution (ABS) was prepared by combining acetic acid and sodium acetate trihydrate. From pH 6.0–8.0, 10 mM, a phosphate buffer solution (PBS) was prepared by combining sodium dihydrogenphosphate dihydrate and disodium hydrogen phosphate dodecahydrate. For pH 8.5–9.0, a 10 mM borate buffer solution (BBS) was prepared by combining sodium tetraborate decahydrate and aqueous sodium hydroxide. These chemicals were purchased from Kanto Chemical Co. (Tokyo, Japan). Bovine serum albumin (BSA), human hemoglobin (Hb), and alpha-chymotrypsin (CHT) were purchased from Sigma-Aldrich Japan Inc. (Tokyo, Japan). Cytochrome C (CytC) was purchased from Nacalai Tesque Inc. (Kyoto, Japan).

B. Preparation of recombinant protein

The recombinant protein intermedilysin (ILY)[25,26] was prepared as follows: The N-terminal hexa-His-tagged recombinant ILY with two point mutations, Gly/83/Cys and Ser/217/Cys, which form a disulfide bond between the Cys residues was prepared by an *Escherichia coli* (*E. coli*) expression system using the expression vector pQE-9 (Qiagen, Hilden, Germany). The expression of recombinant ILY in the *E. coli* transformant was induced in the presence of 1.0 mM isopropyl-β-D-thiogalactopyranoside for 4 h at 37 °C with shaking. After harvesting the grown bacterial cells, the recombinant ILY was extracted from the bacterial cells by sonication and purified using a His-Trap HP column (GE Healthcare, Chicago, IL, USA) on an AKTAprime plus system (GE Healthcare). The purified recombinant ILY was dialyzed in phosphate-buffered saline, and the buffer containing the purified recombinant ILY was changed to assay-buffers composed of 10 mM 2-[4-(2-hydroxyethyl)-1-piperazinyl]ethanesulfonic acid (HEPES) (Dojindo, Kumamoto, Japan) with pH values of 6.5, 7.0, and 8.0.

C. Fabrication of epitaxial graphene FETs

The epitaxial graphene films were grown using a SR1800 rapid thermal annealing system (Thermo Riko, Japan) on the SiC substrate. A 4-in. wafer of semi-insulative 4H-SiC (0001) was purchased from CREE Inc. (Durham, USA). The wafer was cut into $10 \times 10\,mm^2$ SiC substrates and annealed at 1570 °C for 5 min in an Ar atmosphere at 100 Torr. The average sheet resistance, electron concentration, and mobility of the epitaxial graphene films on the SiC substrate were 950 Ω/sq, $7.5 \times 10^{12}\,cm^{-2}$, and $920\,cm^2/(V\,s)$, respectively. These characteristics were sufficiently good and indicate that the epitaxial graphene films were of high quality.[27] The details of the growth conditions and typical uniformity of the epitaxial graphene film on the SiC substrate measured by AFM and Raman mapping were reported in our previous works.[23,27] To measure the electrical characteristics without contact resistance, a conventional Hall bar pattern was formed on the epitaxial graphene film on the SiC substrate. A stencil mask was prepared from a polyethylene terephthalate film cut in a typical Hall bar pattern using a laser beam machine (VD7050, Commax, Japan) and placed on the epitaxial graphene film. The graphene film was removed through conventional air plasma etching. The channel size was $3 \times 3\,mm^2$. After plasma etching, the epitaxial graphene FETs were cleaned using a mixed solution of sulfuric acid and hydrogen peroxide solution and then washed with ultrapure water. Such a strong acid treatment was acceptable because of the stability of the epitaxial graphene film on the SiC substrate.[28]

D. Measurements

A silicone rubber container was placed onto the epitaxial graphene FET to measure the electrical characteristics of epitaxial graphene FETs in various solutions. The buffer solution was then

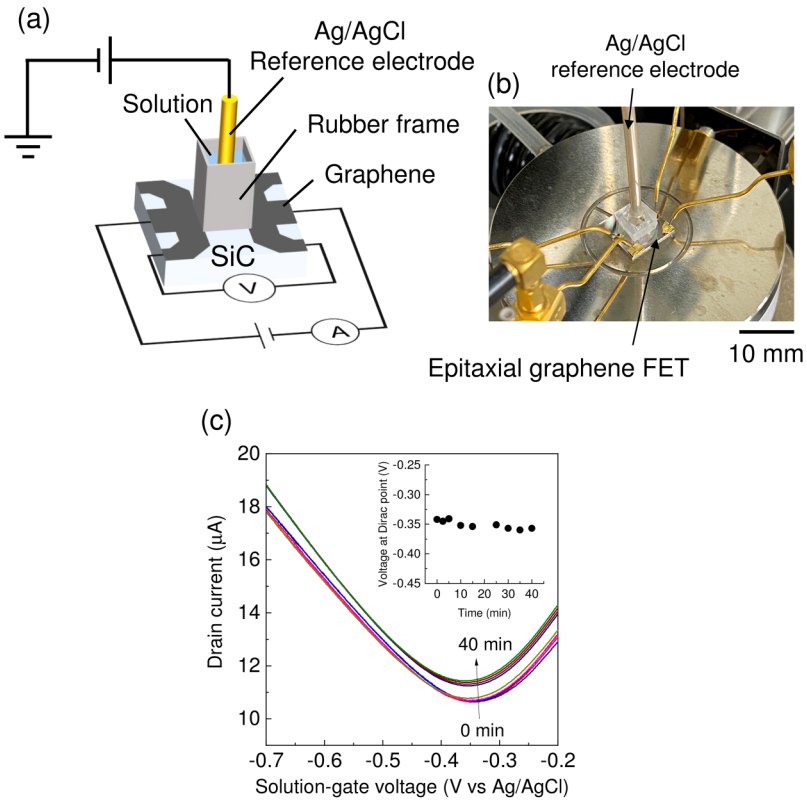

FIG. 1. (a) Schematic illustration and (b) photograph of the measurement setup. (c) I_D–V_G characteristics of epitaxial graphene FETs in the borate buffer solution from 0 to 40 min. The inset shows the time dependence of the charge neutrality point voltage.

poured into the rubber container. An Ag/AgCl reference electrode was inserted into the buffer solution to apply the gate voltage. A reference electrode was used to minimize the environmental effects.[29] The electrical characteristics of epitaxial graphene FETs were measured using a B1500A semiconductor device parameter analyzer (Keysight Technologies, Santa Rosa, USA). Gold foils were placed at the edges of the device, and then probes were placed in contact with the gold foil. It should be noted that the gold foils and probes did not come into contact with the solutions to avoid the leakage current from the metals. As the contact resistance between the metal and epitaxial graphene film was sufficiently small, Ohmic contacts could be obtained using only the metal foil.[24,30] The adsorption of each target protein was measured using different epitaxial graphene FETs. Protein solutions were introduced into the rubber container, and the I_D–V_G characteristics were measured after 5 min. A schematic illustration and photograph of the measurement setup are shown in Figs. 1(a) and 1(b), respectively. All protein adsorption measurements were performed by two different people to ensure reproducibility. For conventional semiconductor FET-based sensors, insulating layers on the channel are required to avoid channel oxidation. However, because the electric potential window of the graphene film was quite large, no insulating layer was needed on the graphene channel.[12]

III. RESULTS AND DISCUSSION

We first confirmed the drift characteristics of epitaxial graphene FETs. Figure 1(c) shows the transfer characteristics (I_D–V_G) of epitaxial graphene FETs in the borate buffer solution (pH 9.0) from 0 to 40 min. The charge neutrality points (Dirac points) were slightly shifted toward negative gate voltages after 40 min ($\Delta V_G < 10$ mV). In other buffer solutions, epitaxial graphene FETs exhibited similar small-drift characteristics. Each concentration-dependent measurement of the I_D–V_G characteristics was carried out within 30 min, and the noise level of the gate voltage shift was lower than approximately 10 mV. At present, the origin of the shift in the current direction is unknown, and the current shift direction differed between the devices; hence, we focused on the shift in the gate voltage direction in this work.

The isoelectric points (pI) of BSA, Hb, CHT, CytC, and ILY were 5.3, 6.8, 8.8, 9.8, and 9.9, respectively. Therefore, these proteins were positively charged in buffer solutions with pH values lower than their pI values, and negatively charged at pH values higher than their pI values. In this study, we prepared positively charged BSA (pH 4.5, 5.0), Hb (pH 6.0, 6.5), CHT (pH 6.8), CytC (pH 7.0), and ILY (pH 6.5, 7.0, and 8.0) and negatively charged BSA (pH 6.0, 6.5, 7.0, and 7.5), Hb (7.0, 7.5, and 8.0), and CHT (pH 9.0) solutions. Because the pI values of CytC and ILY were relatively large (9.8, 9.9), negatively charged solutions of those proteins could not be prepared because solutions with higher pH resulted in their denaturation. Figure 2 shows the I_D–V_G curves of epitaxial graphene FETs in the buffer solutions after introducing various concentrations of positively and negatively charged proteins. Owing to the negative doping of the epitaxial graphene film on the SiC substrate, the charge neutrality points in the buffer

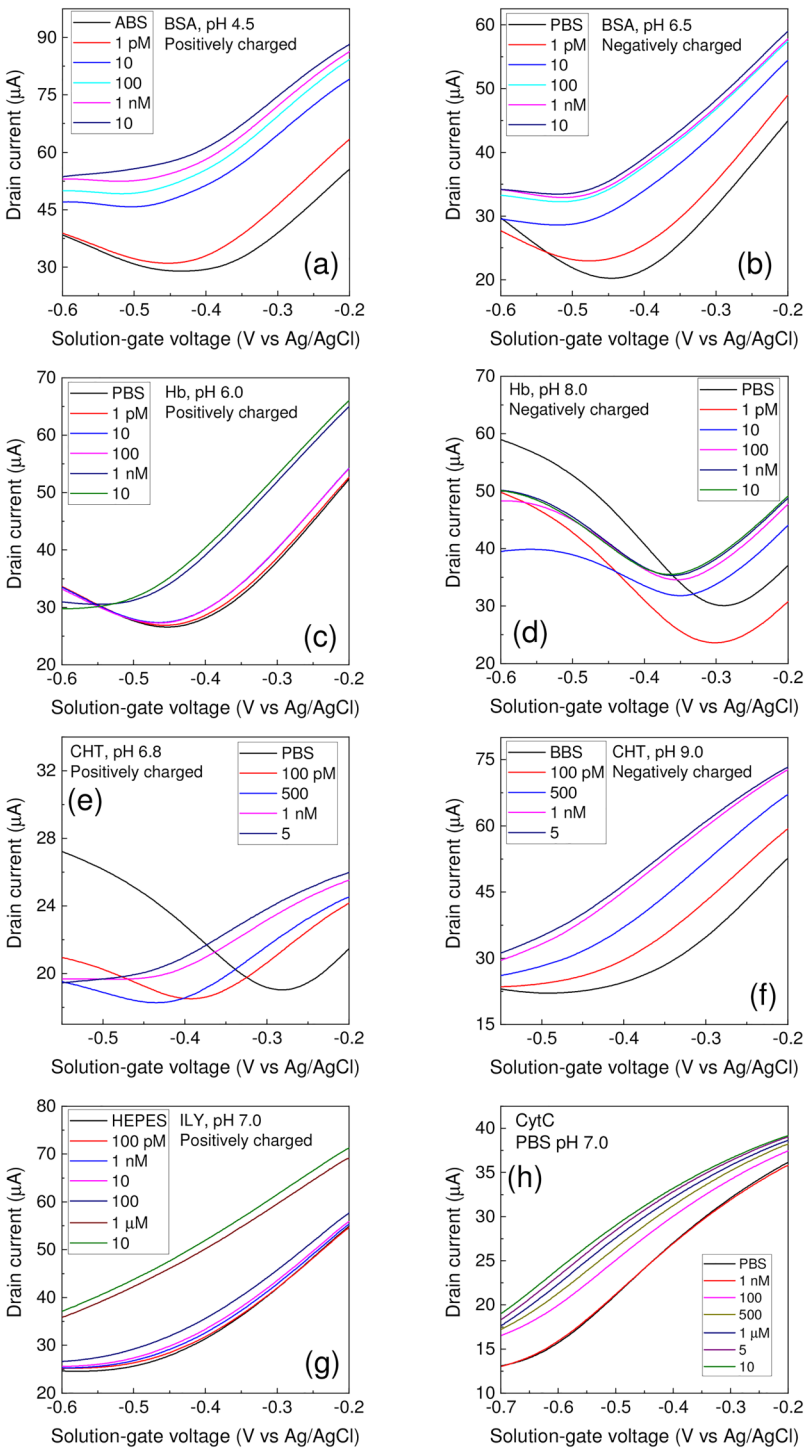

FIG. 2. I_D–V_G characteristics of epitaxial graphene FETs for (a) positively charged BSA at pH 4.5, (b) negatively charged BSA at pH 6.5, (c) positively charged Hb at pH 6.0, (d) negatively charged Hb at pH 8.0, (e) positively charged CHT at pH 6.8, (f) negatively charged CHT at pH 9.0, (g) positively charged ILY at pH 7.0, and (h) positively charged CytC at pH 7.0.

solutions occurred at negative gate voltage values. It should be noted that the voltages at the charge neutrality point in the buffer solution without proteins were different for each sample. These voltage differences were dependent on the carrier concentrations in the epitaxial graphene films. However, epitaxial graphene FETs were insensitive to pH changes owing to their single-crystal characteristics, which resulted in structures with fewer defects and dislocations.[24] To exclude the effects of the change in the charge

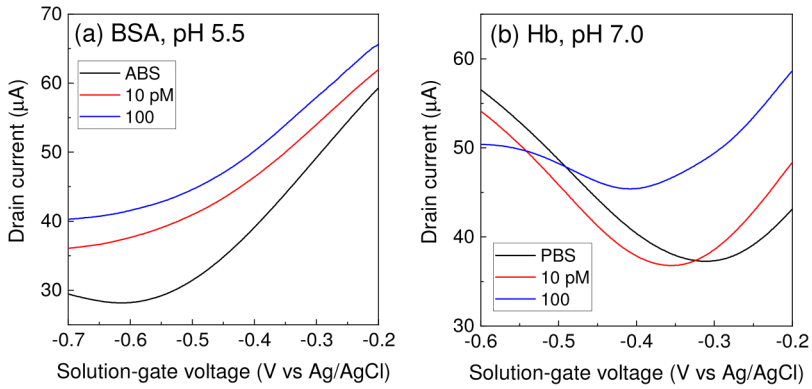

FIG. 3. I_D–V_G characteristics of epitaxial graphene FETs for (a) BSA at pH 5.5 and (b) Hb at pH 7.0. These pH values were very close to the respective pI values.

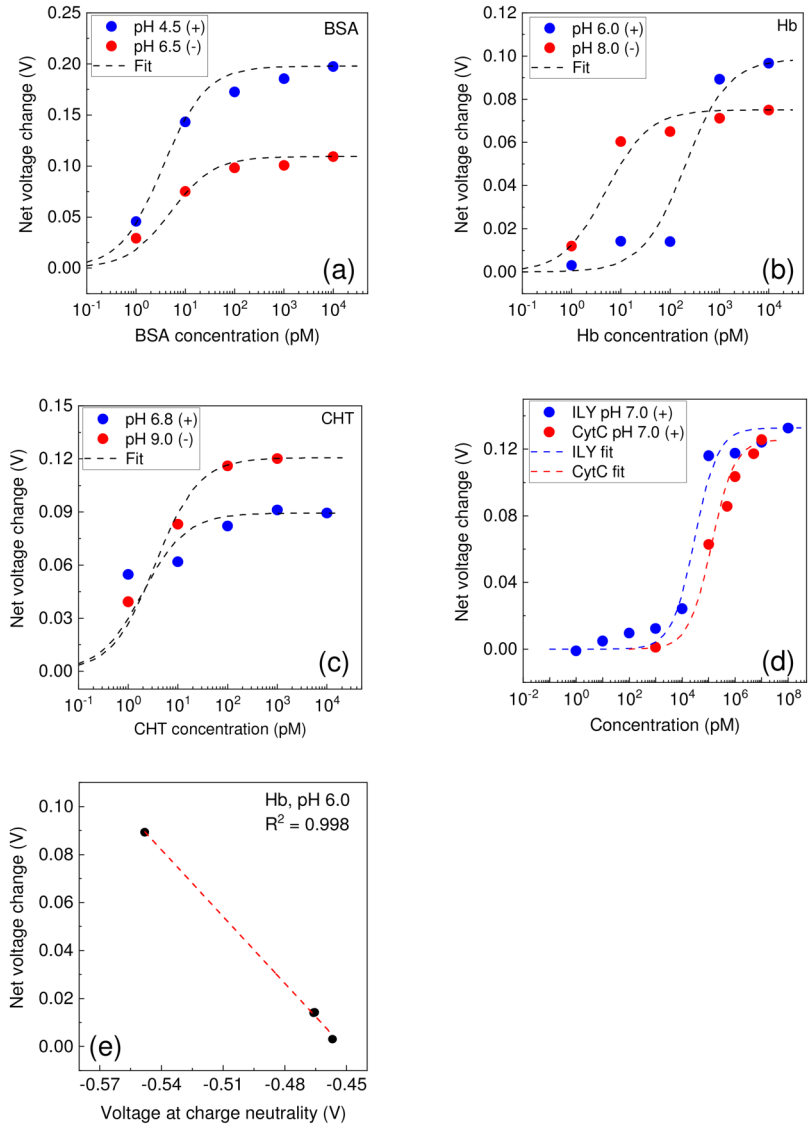

FIG. 4. The net voltage change plotted as a function of protein concentration for (a) BSA, (b) Hb, (c) CHT, and (d) ILY and CytC. The blue and red solid circles indicate positively and negatively charged proteins, respectively. The red dashed lines indicate the Langmuir adsorption isotherm fittings. (e) Net voltage change vs voltage at the charge neutrality point.

neutrality point of each epitaxial graphene FET and the constant voltage (approximately 0.2 V) from the Ag/AgCl electrode, the shift of the gate voltage from the charge neutrality point in the buffer solution due to the change in the carrier concentration with the adsorption of proteins was investigated. All the transfer characteristics of the epitaxial graphene FETs shifted toward the direction of negative gate voltage with increasing protein concentration. These negative voltage shifts were independent of the charge type and pI. Negative voltage shifts were observed at different pH values, indicating that the shift direction was not influenced by the charge condition.

If the electrostatic field effect owing to the charges in the protein was the origin of the shift, the shift direction would be altered when the charge type changed with the pH of the solution. Moreover, such negative voltage shifts would be observed when the solution pH was closest to pI. These trends were indeed observed in the I_D–V_G characteristics of BSA and Hb adsorption at pH 5.5 and 7.0, respectively (Fig. 3). Because pI values of BSA and Hb were 5.3 and 6.8, respectively, the total charge on BSA and Hb was almost zero under these conditions; however, negative voltage shifts with increasing protein concentration were clearly observed. This indicates that the negative voltage shifts from protein adsorption were independent of the amount of charge in the proteins.

To confirm that the I_D–V_G shifts were owing to protein adsorption, the net voltage shifts in the buffer solutions without proteins are plotted as functions of the protein concentration [Figs. 4(a)–4(d)]. The most robust method is to plot the relative gate voltage values at the charge-neutrality points of I_D. However, the charge neutrality points were often not observed because of the negative doping due to protein adsorption and the distortion of the I_D–V_G characteristics due to charge transfer from the proteins. Therefore, the net voltage shifts were estimated from the I_D change (ΔI_D) normalized by the transconductance ($g_{m,max}$; the maximum value of the slope),[31] using the value of ΔI_D at $g_{m,max}$. To confirm the validity of this calibration, the typical variation of the charge neutrality point with the net voltage change was plotted and found to exhibit good linear characteristics, as shown in Fig. 4(e). All the net voltage shifts increased rapidly at low protein concentrations and saturated at higher concentrations [Figs. 4(a)–4(d)]. These characteristics can be described using the Langmuir adsorption isotherm

$$\Delta V_G = \frac{\Delta V_{G,\,max} \cdot C}{C + K_D}, \tag{1}$$

where ΔV_G, $\Delta V_{G,\,max}$, C, and K_D are the net voltage change, the maximum value of the net voltage change, protein concentration, and dissociation constant, respectively. The dashed lines in Fig. 4 represent the fitting curves. The trend of all the net voltage shifts at various pH values fits well with the Langmuir adsorption isotherm, indicating that these voltage shifts were due to protein adsorption. A slight difference in the maximum net voltage changes between negatively and positively charged proteins is observed in Fig. 4. We believe that the adsorption characteristics of the amino acids would be needed to clarify the origin of this difference.

The shift directions and voltage values of the positively and negatively charged proteins are shown in Fig. 5. The average shift

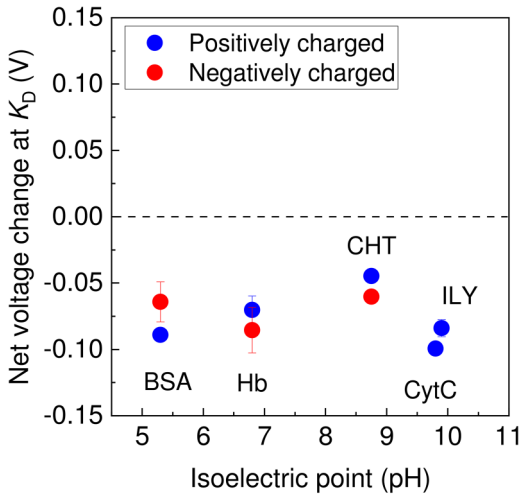

FIG. 5. Gate voltage shifts at the K_D protein concentrations obtained from the Langmuir adsorption isotherm fitting curves. The error bars indicate the standard deviation.

voltage values were obtained from the Langmuir adsorption isotherm curves at the concentration K_D, which is the concentration at which 50% coverage of the epitaxial graphene surface occurred. Negative voltage shifts were exhibited in all the results because of the electron doping induced by protein adsorption. Moreover, the net voltage shifts had very similar values over a wide range of pI values. These results indicate that the influence of protein adsorption on the electrical properties of the epitaxial graphene film are independent of pI, pH, and charge type. These phenomena cannot be explained by the electrostatic field effect but only by charge transfer from the protein to the epitaxial graphene film. In reality, the adsorbed proteins may not be actually ordered into a monolayer because of the slight errors in the fitting curves; hence, the I_D–V_G shift may have originated from additional causes besides charge transfer. However, we believe that the main origin of the I_D–V_G shift is the charge-transfer effect.

There have been several theoretical and experimental studies on charge transfer in graphene films by molecule adsorption. For example, Coletti *et al.* reported the observation of electron doping by tetrafluoro-tetracyanoquinodimethane adsorption using angle-resolved photoemission spectroscopy.[18] Qin *et al.* reported density functional theory (DFT) calculations of the interactions between L-leucine and the graphene surface and found that the electronic structure of graphene can be controlled by the orientation of L-leucine.[17] Rodríguez *et al.* reported DFT calculations of amino acid adsorption on graphene and the transfer of charge from the graphene to the molecules due to substrate–adsorbate interactions.[19] In this study, the shift direction was independent of the charge type and amount. This result contradicts the findings in other works on charge transfer-type protein detection.[14,20] Although further investigations are needed, we consider the orientations of the proteins on the epitaxial graphene film to be almost identical because of the absence of defects, dislocations, and

TABLE I. The obtained K_Ds for protein adsorption onto various graphene films.

Specimen	Graphene	K_D (M)	Reference
BSA	Epitaxial	2.8×10^{-11}	This work
Hb	Epitaxial	5.5×10^{-11}	This work
CHT	Epitaxial	2.6×10^{-12}	This work
CytC	Epitaxial	1.3×10^{-7}	This work
ILY	Epitaxial	1.4×10^{-8}	This work
BSA	Exfoliation	1.5×10^{-8}	Ref. 12
Dopamine	rGO	$\sim 4 \times 10^{-3}$	Ref. 32
Dopamine	CVD	$\sim 7 \times 10^{-7}$	Ref. 33

polymer residues. This may have resulted in some selectivity in the binding part of the proteins and leads to stable electron doping even when the charge type and amount differed. These results indicate that protein adsorption on an epitaxial graphene film leads to stable charge transfer (electron doping) characteristics.

Finally, the obtained average K_D values for each molecule using epitaxial graphene FET-based sensors were compared to those obtained using sensors with graphene synthesized through mechanical exfoliation, rGO, and CVD (Table I). In this table, only the simple physisorption characteristics are summarized. The K_D values obtained, except those of CytC and ILY, are much smaller than those reported.[12,32,33] Because both CytC and ILY showed larger K_Ds, it can be concluded that the epitaxial graphene film is insensitive to proteins with high pI values. However, the smaller K_D for proteins with lower pI values implies that epitaxial graphene FETs have higher sensitivity than those other graphene-based FETs. A smaller K_D may also increase the noise intensity. The suppression of non-specific adsorption on epitaxial graphene on the SiC substrate is very important for receptor-modified epitaxial graphene FETs. Such non-specific adsorption can be suppressed by molecule modification.[34] For practical sensor devices, the combination of receptors and blocking molecules is crucial. The stability of the changes in the electrical characteristics resulting from protein adsorption on epitaxial graphene on SiC substrates indicates that the inherent protein adsorption characteristics on the graphene film are independent of the charges in the proteins.

IV. CONCLUSIONS

The protein adsorption characteristics of the epitaxial graphene film were investigated. Single-crystal epitaxial graphene-based FETs were fabricated using a resist-free fabrication process to eliminate the effects of polymer residues. Five kinds of proteins with various pI values at various pH values were injected onto epitaxial graphene FETs. All the I_D–V_G curves exhibited shifts in the direction of negative gate voltages. The shift direction was independent of pI and pH, indicating that the sign of the protein charges was not the main origin of the shift in the graphene FET-based sensors. We concluded that the inherent protein adsorption mechanism did not cause the electrostatic field effect but rather charge transfer (electron doping). Moreover, K_D values of the proteins obtained using epitaxial graphene FETs were more than 100 times smaller than those obtained using other graphene sensors. This indicates that the charge transfer-type epitaxial graphene-based biosensors have significant potential as highly sensitive biosensors compared to graphene-based sensors fabricated by other synthesis methods and can be used as a reference standard for graphene-based biosensors.

ACKNOWLEDGMENTS

This work was supported by JSPS KAKENHI (Grant Nos. JP19H02582, JP18K09552, and JP21H01394). We would like to thank Editage (www.editage.com) for English language editing.

DATA AVAILABILITY

The data that support the findings of this study are available from the corresponding author upon reasonable request.

REFERENCES

[1]A. K. Geim and K. S. Novoselov, Nat. Mater. **6**, 183 (2007).
[2]K. S. Novoselov, A. K. Geim, S. V. Morozov, D. Jiang, Y. Zhang, S. V. Dubonos, I. V. Grigorieva, and A. A. Firsov, Science **306**, 666 (2004).
[3]K. S. Novoselov, A. K. Geim, S. V. Morozov, D. Jiang, M. I. Katsnelson, I. V. Grigorieva, S. V. Dubonos, and A. A. Firsov, Nature **438**, 197 (2005).
[4]C. Lee, X. Wei, J. W. Kysar, and J. Hone, Science **321**, 385 (2008).
[5]K. I. Bolotin, K. J. Sikes, Z. Jiang, M. Klima, G. Fudenberg, J. Hone, P. Kim, and H. L. Stormer, Solid State Commun. **146**, 351 (2008).
[6]S. Afsahi, M. B. Lerner, J. M. Goldstein, J. Lee, X. Tang, D. A. Bagarozzi, D. Pan, L. Locascio, A. Walker, F. Barron, and B. R. Goldsmith, Biosens. Bioelectron. **100**, 85 (2018).
[7]J. Sethi, M. V. Bulck, A. Suhail, M. Safarzadeh, A. Perez-Castillo, and G. Pan, Microchim. Acta **187**, 288 (2020).
[8]D. K. H. Tsang, T. J. Lieberthal, C. Watts, I. E. Dunlop, S. Ramadan, A. E. D. R. Hernandez, and N. Klein, Sci. Rep. **9**, 013946 (2019).
[9]Y. Taniguchi, T. Miki, Y. Ohno, M. Nagase, Y. Arakawa, and M. Yasuzawa, Jpn. J. Appl. Phys. **58**, SDDD02 (2019).
[10]C. W. Chen, S. C. Hung, M. D. Yang, C. W. Yeh, C. H. Wu, G. C. Chi, F. Ren, and S. J. Pearton, Appl. Phys. Lett. **99**, 243502 (2011).
[11]G. Chen, T. M. Paronyan, and A. R. Harutyunyan, Appl. Phys. Lett. **101**, 053119 (2012).
[12]Y. Ohno, K. Maehashi, Y. Yamashiro, and K. Matsumoto, Nano Lett. **9**, 3318 (2009).
[13]Y. Ohno, K. Maehashi, and K. Matsumoto, Biosens. Bioelectron. **26**, 1727 (2010).
[14]S. Chen, Y. Sun, Y. Xia, K. Lv, B. Man, and C. Yang, Biosens. Bioelectron. **156**, 112128 (2020).
[15]L. Zhou, K. Wang, Z. Wu, H. Dong, H. Sun, X. Cheng, H. L. Zhang, H. Zhou, C. Jia, Q. Jin, H. Mao, J. L. Coll, and J. Zhao, Langmuir **32**, 012623 (2016).
[16]S. Wang, M. Z. Hossain, K. Shinozuka, N. Shimizu, S. Kitada, T. Suzuki, R. Ichige, A. Kuwana, and H. Kobayashi, Biosens. Bioelectron. **165**, 112363 (2020).
[17]W. Qin, X. Li, W. W. Bian, X. J. Fan, and J. Y. Qi, Biomaterials **31**, 1007 (2010).
[18]C. Coletti, C. Riedl, D. S. Lee, B. Krauss, L. Patthey, K. von Klitzing, J. H. Smet, and U. Starke, Phys. Rev. B **81**, 235401 (2010).
[19]S. J. Rodríguez, L. Makinistian, and E. A. Albanesi, Appl. Surf. Sci. **419**, 540 (2017).
[20]S. Ghosh, N. I. Khan, J. G. Tsavalas, and E. Song, Front. Bioeng. Biotechnol. **6**, 29 (2018).
[21]S. Tanabe, Y. Sekine, H. Kageshima, M. Nagase, and H. Hibino, Appl. Phys. Express **3**, 075102 (2010).
[22]H. Kuramochi, S. Odaka, K. Morita, S. Tanaka, H. Miyazaki, M. V. Lee, S.-L. Li, H. Hiura, and K. Tsukagoshi, AIP Adv. **2**, 012115 (2012).

[23]Y. Ohno, Y. Kanai, Y. Mori, M. Nagase, and K. Matsumoto, Jpn. J. Appl. Phys. **55**, 06GF09 (2016).
[24]T. Mistuno, Y. Taniguchi, Y. Ohno, and M. Nagase, Appl. Phys. Lett. **111**, 213103 (2017).
[25]H. Nagamune, C. Ohnishi, A. Katsuura, K. Fushitani, R. A. Whiley, A. Tsuji, and Y. Matsuda, Infect. Immun. **64**, 3093 (1996).
[26]A. Tabata, Y. Ohkubo, E. Sakakura, T. Tomoyasu, K. Ohkura, and H. Nagamune, Anticancer Res. **32**, 2323 (2012).
[27]T. Aritsuki, T. Nakashima, K. Kobayashi, Y. Ohno, and M. Nagase, Jpn. J. Appl. Phys. **55**, 06GF03 (2016).
[28]T. Kujime, Y. Taniguchi, D. Akiyama, Y. Kawamura, Y. Kanai, K. Matsumoto, Y. Ohno, and M. Nagase, Phys. Status Solidi B **257**, 1900357 (2019).
[29]E. D. Minot, A. M. Janssens, I. Heller, H. A. Heering, C. Dekker, and S. G. Lemay, Appl. Phys. Lett. **91**, 093507 (2007).
[30]M. Nagase, H. Hibino, H. Kageshima, and H. Yamaguchi, Appl. Phys. Express **3**, 045101 (2010).
[31]F. N. Ishikawa, M. Curreli, H. K. Chang, P. C. Chen, R. Zhang, R. J. Cote, M. E. Thompson, and C. Zhou, ACS Nano **3**, 3969 (2009).
[32]Q. He, H. G. Sudibya, Z. Yin, S. Wu, H. Li, F. Boey, W. Huang, P. Chen, and H. Zhang, ACS Nano **4**, 3201 (2010).
[33]M. Zhang, C. Liao, Y. Yao, Z. Liu, F. Gong, and F. Yan, Adv. Funct. Mater. **24**, 978 (2014).
[34]Y. Taniguchi, T. Miki, Y. Ohno, M. Nagase, Y. Arakawa, Y. Imada, K. Minagawa, and M. Yasuzawa, Jpn. J. Appl. Phys. **58**, 055001 (2019).